Petroleum and Coal

Augmented Wireline Based Lithology and Facies Prediction, for Upper Ordovician Succession, Murzuq Basin, Libya

Abubaker Alansari[1]*, Ahmed Mohammad Ahmed Salim[1], Abdul Hadi Bin Abd Rahman[1], Nuri Mohamed Fello[2], Hammad Tariq Janjuhah[3]

[1] *Department of Geosciences, University Technology PETRONAS, 32610, Perak, Malaysia*
[2] *National Oil Corporation (NOC), Tripoli, Libya*
[3] *Department of geology, American University of Beirut, Libanon*

Abstract

The upper Ordovician reservoir is one of the leading producing units in SW part of the Murzuq basin; it has a complex architecture inherited from the glacial effects on the braided fluvial deposits of the late stage at this era. The ultimate target for any petrophysical evaluation is to determine the quantities of water saturation and porosity accurately, but unfortunately, the models for thinly interbedded sand and shale layers are not straightforward. Therefore in this paper, an effort has been made to delineate and distinct between the types of interbedded (shaly-sand and sandy-shale layers), and lithology end members by application compressional compliance versus density cross-plot in the two studied wells. After that, the determination of the thinly interbedded of layers type is augmented by correlating Vp-compliance with Poisson's ratio, effective porosity, and VP/VS. Among all the examined cross-plot; Poison's ratio, VP/VS and effective porosity with compressional compliance enhanced the upper and lower boundaries of the thinly interbedded sand and shale layers of the Ordovician succession in Murzuq basin. The "Mamuniyat" formation (main reservoir) with more clean sand content displays low compressional compliance, low-velocity ratio, and low Poisson's ratio. In contrary, the rich TOC shale (Hot shale) shows high compressional compliance, high-velocity ratio and high Poisson's ratio. While the disputed sandstone, siltstones and silty shales of late Ordovician "Bir Tlacsin" formation has slightly higher compressional compliance, velocity ratio, and Poisson's ratio than the underlying Mamuniyat formation, which enables drawing a clear contact between two gradually graded formations in the areas with no abrupt changes. The estimated petrophysical and elastic and properties are then used as an input for electrofacies prediction in both wells, by using unsupervised neural network classification. The predicted petrophysical facies clusters in both wells failed to differentiate between the various type of shales. However, the petro-elastic facies cluster reliably delineated the interbedded sandy - shale and shaly-sand thin layers without using gamma-ray logs. The results will help to avoid and to reduce the errors made during fluid substitution and rock physics models of shaly-sand formations.

Keywords: *Lithology prediction; Electrofacies; Upper Ordovician reservoir; Murzuq Basin.*

1. Introduction

A principal task of geoscience in reservoir characterization is to determine the diverse lithofacies and elactrofacies clusters of the main zone of interest from the interpretation of wireline and cores obtained from wells. However, for technical and financial causes cores are not always derived for the entire reservoir zone. Besides In old exploration wells, greatly deviated and horizontal wells only wireline data are often available. Thus petrophysical properties, elastic properties, lithology, and facies prediction depend on the interpretation of the wireline logs. With the advent of quantitative seismic interpretation and rock physics modelling been incorporated into the conventional hydrocarbon exploration appraisal and development workflow, it became a necessity to understand the minor component of the reservoir unit. The upper

Ordovician reservoir are the main producing unit in the study area SW part of the Murzuq basin (Fig. 1); it has a complex architecture which has been inherited from the glacial effects on braided fluvial deposits during the Ordovician time.
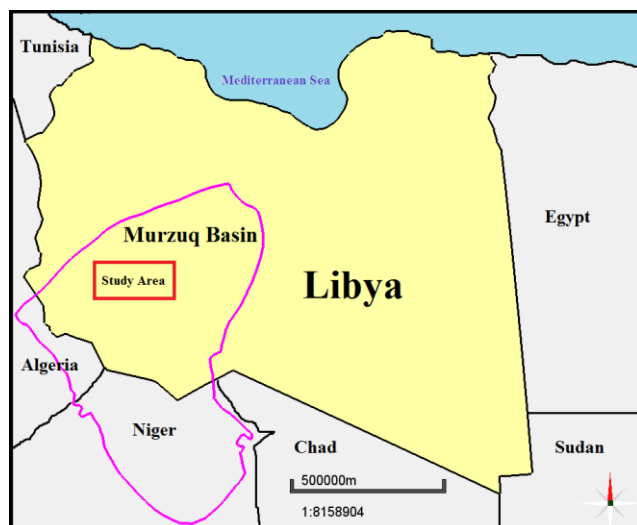

Fig. 1. Location of studied wells, Murzuq Basin, Libya

Consequently, there is no consistency on the lithostratigraphic units that constitute the Ordovician sedimentary infill of the Murzuq Basin. Especially the transitional deposits between the source rock formation and underlying reservoir units that remains accurately undefined [1], They also consider this unit (Bir Tlacsin formation) as non-reservoir rocks which baffles the hydrocarbon flow during migration and production process. Furthermore, the thinning and gradually graded contacts with upper and lower formations masks the identification of this formation boundaries, consequently top reservoir boundary. In the literature, there is an obvious gab in the studies concerned with the use of wireline data to overcome the fore stated problem in this region. A recent study by Abushalah and Serpa [2] have defined the upper and the lower boundary of this formation using seismic amplitude spectrum analysis and inverted density attributes, however, the density the Bir Tlacsin formation overlaps with densities of Mamuniyat and Tanezzuft formation even at wells scale. According to Bhat and Helle [3] the large overlap of the petrophysical properties in clastic rocks limit their effectiveness in accurate facies prediction. Therefore, in-depth integrated petrophysical and elastic analysis to comprehend the lithology end members and facies is required before seismic inversion and reservoir modelling.

According to [4-5], the mixed shale-sand layers should lie in a straight line between the two parent lithology end members (sand and shale). The former [4] has proposed workflow for determining shaly-sand lamination based on VP-compliance and density for a better application of fluid substitution, while the latter [5] improved the interpretation of the fluid substitution models. By modelling the volume of dispersed shale, and its correlation with effective porosity VP. In this paper, the above method has been adopted and developed to enable the delineation of the existence of shaly-sand and sandy-shale layers distribution at the reservoir and well scale through incorporating more petro-elastic correlation applied to study wells. The principal objective of this paper is; 1) to determine the petro-elastic properties of the main lithology end members of the Upper Ordovician reservoir unit. 2) To enhance the separation of inter-bedded sandy-shale and shaly-sand layers by minimizing the overlap between petrophysical properties of different fluid cases within the zone of interest. 3) Finally, group them into electro-facies derived from both petrophysical and elastic properties.

2. Geological settings

Ordovician reservoirs and their main lithofacies have been investigated in the recent geological record by many researchers namely [6-11]. Based on these studies the Ordovician plays were divided into several underlying sub-groups, but in this paper, the focus will be a shift to upper Ordovician deposits (Fig. 2).

2.1. Upper Ordovician

According to Aziz [6] Najem *et al.* [9] ,El-Ghali [11], Shalbk [12] during the Late Ordovician, Melaz Shuqran Mamuniyat, and Bir Tlacsin formations were alternately deposited and locally covered by the basal Silurian marine deposits. The main Ordovician reservoir (Mamuniyat

formation) is typified by three sand-dominated cycles that indicate complex interlace of marine and glacial depositional effects (Fig. 2). The Lower Ordovician reservoirs consist of 3 zones, which are discussed below:

Fig. 2. Representing the upper Ordovician lithostratigraphic column of the studied area (*Modified from* [11])

Lower Mamuniyat: This zone comprises the marine and possibly glacially-influenced Melaz Shuqran Formation, which was typically deposited in shallow to marginal marine settings (Fig. 2). Middle Mamuniyat: This zone covers the Middle Mamuniyat sequence with the deposition of proximal braid deltas. Some studies such as suggest deposition into glacial lakes/ponds that accumulated in ice-formed valleys and may be subjected to a marine transgression. Glacial influence is believed to be the toughest in this zone likened to the others (Fig. 2). Upper Mamuniyat: This zone includes the Upper Mamuniyat series, which typically contains upward coarsening braid-delta and localized shallow marine deposition with glacial influences. Localized burrowing (including Skolithos) testifies to the marine-influenced in this zone, which is

typically represented by sub-aqueous deposition of deltas which prograded from glacial sources. The zone is terminated by coarse braid delta deposition and the localized reworking of some deposits by possible aeolian processes. This is typically overlain by a transgressive phase and marine reworking. The contact with the overlying marine Silurian is characteristically distinctive, and may also be unconformable (Fig. 2). Reservoir quality of the Mamuniyat formation is maximum in the medium- to very coarse-grained fluvial sandstones with porosity up to 25% and permeability commonly up to 1000 mD (but locally higher). The glacially-influenced sandstones show reduced reservoir quality, possibly as a result of poorer sorting characteristics.

3. Methodology

Two wells were used for deriving the main petrophysical and elastic properties. Then both properties have been combined using multiple cross-plots to delineate the Lithology end members (sand, shale, sand-shale and shale-sand layers). After that, a set of selected petrophysical and petro-elastic properties have been imported to the unsupervised neural network for electrofacies prediction.

3.1. Petrophysical interpretation

Two wells had relevant wireline logs that include Gamma-ray (GR), Resistivity, Sonic, Neutron and Density logs from which the volume of shale, porosity and water saturation were derived. For V-shale estimation the Linear GR method will be used after best determination GRmax and GRmin using the following equation; For porosity determination, a combination method of neutron porosity, density and sonic logs will be applied to obtain more favourable total porosity (φ total) [13]. After that total porosity will be obtained by using the weighted average of neutron density porosity. The result was also supported by neutron density method. For effective porosity derivation [14] will be used by combining results. Finally, for water saturation estimation Indonesian equation have been used.

3.2. Elastic properties determination

Fortunately, in all the wells compressional sonic log is available but the shear wave sonic exist in only one well. Several methods will be used for Vs estimation, these methods included Castagna "mudrock line", Greenberg-Castagna, correlation regressions and finally multi-set of well logs as an input for supervised neural network method. After that, the above methods will be compared, and one of them will be selected based on its accuracy when compared to the measured Vs from well A. Gassmann fluid substitution is often employed on estimating elastic properties of clean sands with different water saturation for different fluid types and with a different range of porosities. For this paper shaly-sand, the fluid substitution will be applied to well A and B using the average reservoir porosity and pressure values. The mass balance equation will be used for calculating the bulk density of the mixed fluid rock. Moreover, fluid modulus has been estimated by using Wood's

3.3. Compressional-compliance to determination

For defining the main end members of clastic lithology, we will be using the equation suggested by Kathara [4], Backus [15].

$$\rho_1 = \rho_{Sh} * X_{Sh} + \rho_{SD} * (1 - X_{Sh}) \tag{1}$$

$$\frac{1}{\rho V p^2} = \frac{X_{Sh}}{\rho_{Sh} * V p_{Sh2}} + \frac{1 - X_{Sh}}{\rho_{SD} * V p_{SD2}} \tag{2}$$

where ρ = density; Vp is velocity; Sh = shale and subscript SD denotes sand.

The above two equations infer that both density and the compressional compliance (C=1/(ρVp^2)), are linear functions of shale fraction. Which helped on the initial determination of interbedded sand and shale layers within the reservoir unit. Furthermore, the fluid substituted cases will be plotted against compressional compliance. Hence it is expected to provide more lithology separation especially, for the clean sand gas unit.

3.4. Facies prediction

Finally, the estimated petrophysical and elastic and properties has been used as an input for electrofacies prediction in both wells, by using unsupervised neural network classification. Two inputs will be used; first, petrophysical logs only (GR, NPHI, ROHB and PHI) as an input and it was called petrophysical facies. The second a combination of elastic and petrophysical properties (Poison's ratio, VPVS and effective porosity with compressional compliance), named petro-elastic. Then both facies will be calibrated to litho-facies derived from mud logging and wellbore side-cutting reports. The facies associations will be grouped to fit the facies association introduced by [16]

4. Results

4.1. Shear wave estimation (VS)

Three methods were tested for shear velocity prediction (VS) in well B, and then compared to the measured Vs in Well-A (Fig. 3). The estimated shear velocity using supervised neural networks (blue curves) illustrated an excellent overlap with the measured (VS) represented by the red colour curve in both wells. The result was achieved by using an input of gamma-ray, effective porosity, Compressional compliance, and density logs in a supervised neural network with three hidden layers. While the other two curves represent derived Greenberg-Castagna (black colour) and linear regression resulted from correlating VP measured and Vs measured (dotted purple colour) (Fig. 3). The former is slightly higher than measured shear velocity and slightly different from the other curves. Similarly the latter is noticeably lower than measured Vs (Fig. 3).
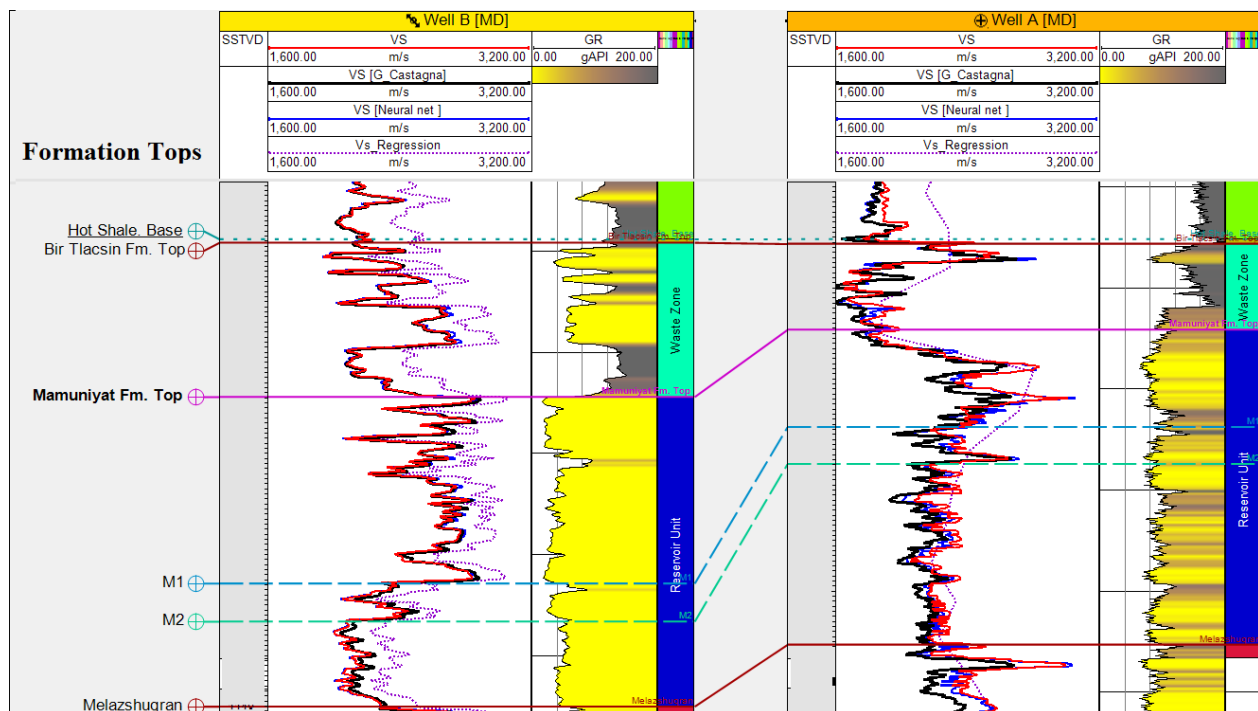

Fig. 3. Vs prediction using three methods in Well A and Well B. (B). Red colour reflecting measured VS value, whereas the black colour representing Greenberg-Castagna derived VS, blue colour denotes the neural-network, and dotted purple is shear velocity estimated using the regression values with VP

4.2. Shale and sand end members' determination

Compressional compliance has been estimated for main reservoir intervals, and entire the wells (A and B) by using the workflow explained in section 3.2.3. Before starting the analysis

of defining shale and sand lithology end members, their distribution should be solely understood. Therefore, the volume of shale log (X) was cross-plotted against gamma-ray log (Y) and colour-coded by total porosity in the reservoir zone for both wells (Fig. 5). It showed that; the clean sand cut-off in both wells has ranged between (0 – 0.3) shale percentage in both wells and shale zone considered to be all the values which more than 0.75. The minimum gamma reading in well A is higher than the one in well B (20 to 60 API) and (67 to 110 API) respectively, which means that the gamma-ray log is not reliable lithology represented in well in well A.
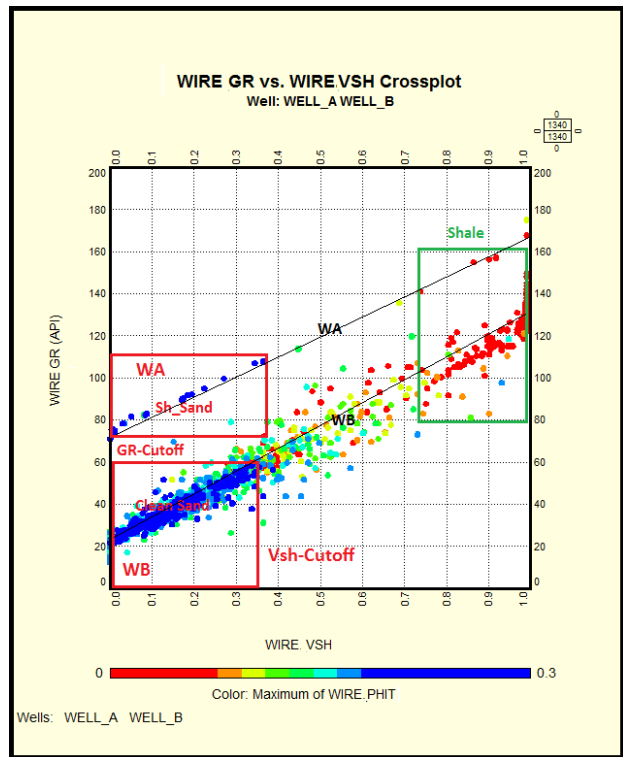

Fig. 4. A cross plot of V-shale and gamma-ray to determine the clean sand and shale cut-off
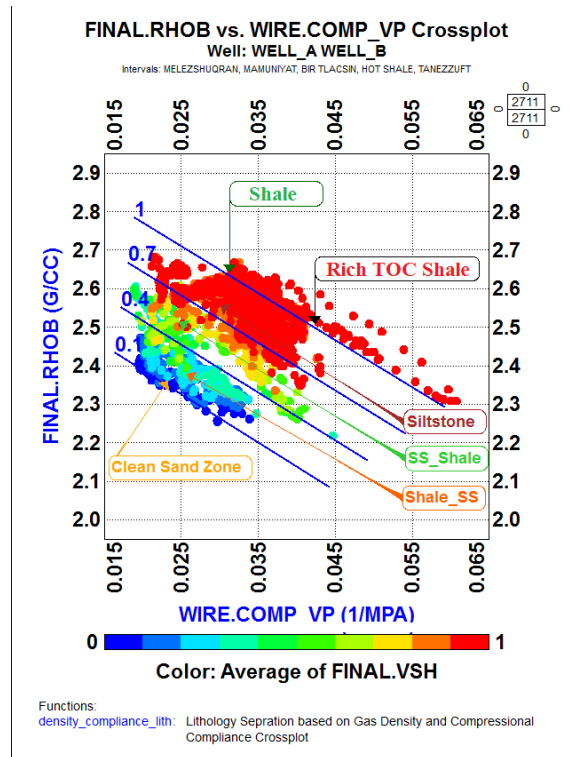

Fig. 5. A cross plot of compressional compliance versus the density (colour-coded by V-shale) reflecting the two main lithology end members (sand is blue and shale red) for the zone of interest in both Wells

4.3. Compressional compliance versus density cross-plot

Once the primary lithology distribution is understood at both wells, the resulted compressional compliance was correlated with density log in both wells (A & B) and colour-coded by the volume of shale (V-Sh). For each cross plot, a function representing the percentage of shale within the sandy layers is drowned with a range of (0 Sand-1 Shale) and an interval of 0.3.

Figure (5) illustrates a cross plot of compressional compliance vs density log annotated by lines showing the percentages of shale in each formation. Where any values higher than 1% considered to be pure shale, more than 0.7% and less than 1% is siltstone with mud layers, between 0.4 and 0.7% is interpreted to be a sandy shale layer. While the lithology points fell below 0.4% and higher than 0.2% is considered to be shaly- sand layers and any percentages lower than that is clean sand (Fig. 5). The lithology end members showed a distinct trend in both wells at the reservoir interval with a very some mixed layers in between (Fig.5).

The above-stated separation is increased when the density of oil used and even more by using the density of gas curve, which has enabled a better selection of the primary lithology end members (sand and shale) and their associated mixed layers (sand-shale and shale-sand)

in both wells (Fig. 6). However, with the remaining uncertainty that associated with an allocation of the contact between sand-shale and shale-sand layers.
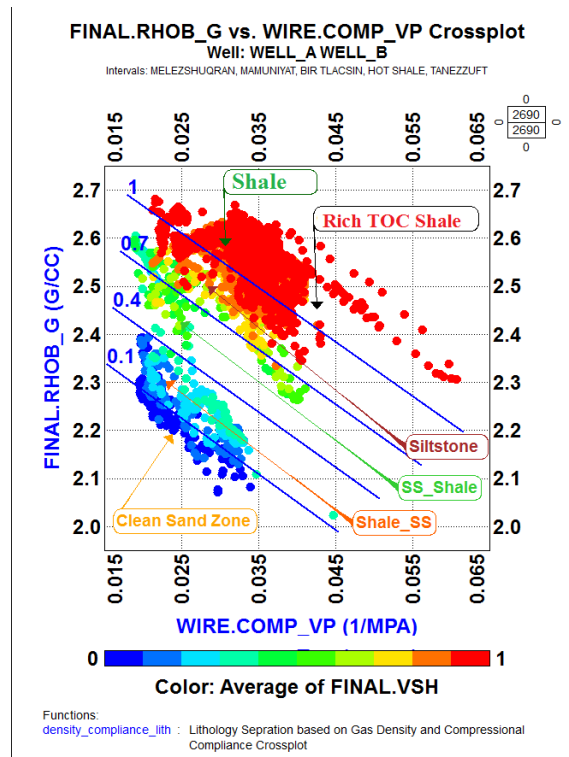

Fig. 6. A cross plot of compressional compliance versus the density of gas case (colour-coded by V-shale) reflecting the two main lithology end members (sand is blue and shale red) for the zone of interest in both Wells
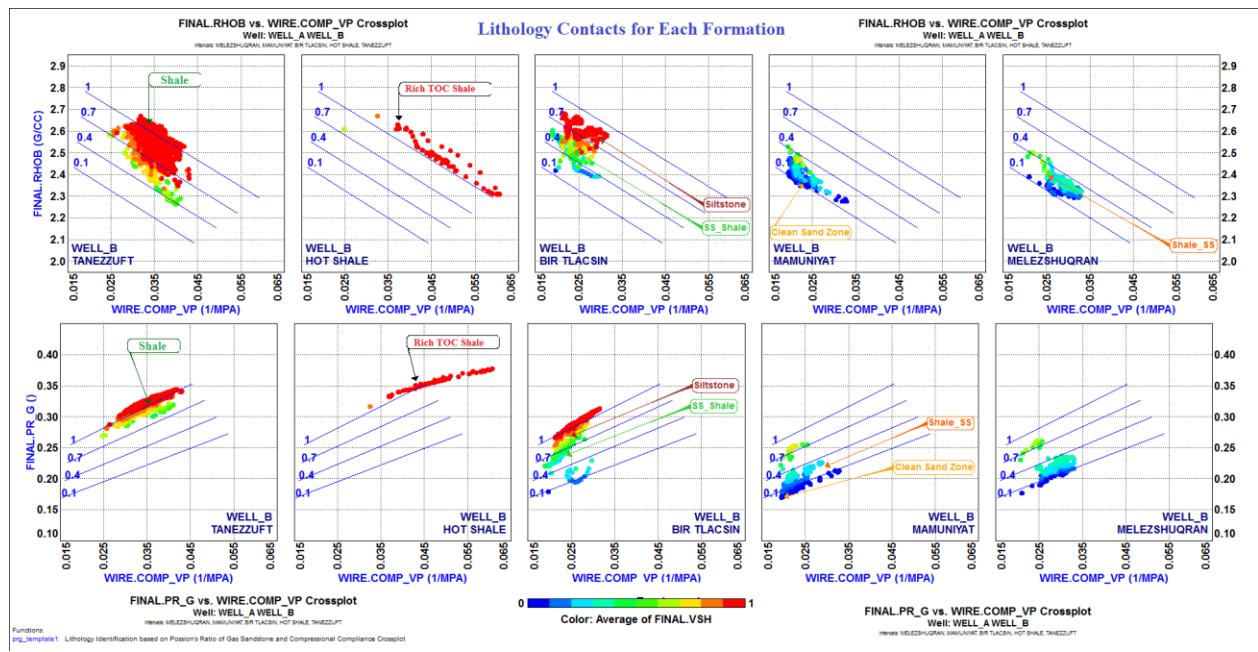

Fig. 7. Compressional compliance versus density cross-plots for each formation within the within the zone of interest, (colour-coded by V-shale) reflecting the percentages and lithology type in both studied wells

To comprehend the composition in the zone of interest, the main formations were investigated individually (Fig. 7). The pure shale (Tanezzuft Silurian shale) annotated by red colour can be outlined in Well A between density range of 2.5 to 2.66 G/CC, and compressional compliance of 0.025 to 0.043 1/MPA. The shalness of the formation in well A is higher than Well B. The cross-plot also enabled an accurate delineation of the rich TOC shale "Hot shale" especially in well B where the formation is characterized with higher compliances and gradual decrease in the density (Fig. 7). The next formation (Bir Tlacsin) is more complicated than others since it contains a range of rock types (shale, siltstone, and mixed shale sand layers) which harden the lithology and facies interpretation of this formation and often confused with upper shale unit (Tanezzuft) and lower reservoir unit (Mamuniyat).

The main reservoir unit (Mamuniyat) showed by dark to light blue colours in both wells; the formation has similar density values with the underlying lower Ordovician formation (Melezshuqran). However, with a definite difference in the compliance values than the lower Mamuniyat reservoir. The Mamuniyat lithology points range lower than 0.026 1/MPA, while Melezshuqran is higher.

4.4. Effective porosity versus compressional compliance cross-plot

Another way for improving the lithology prediction and contacts allocation between different formations at the well scale is to cross-plot the corrected effective porosity vs estimated compressional compliance colour-coded by average shale volume curve (Fig. 8).
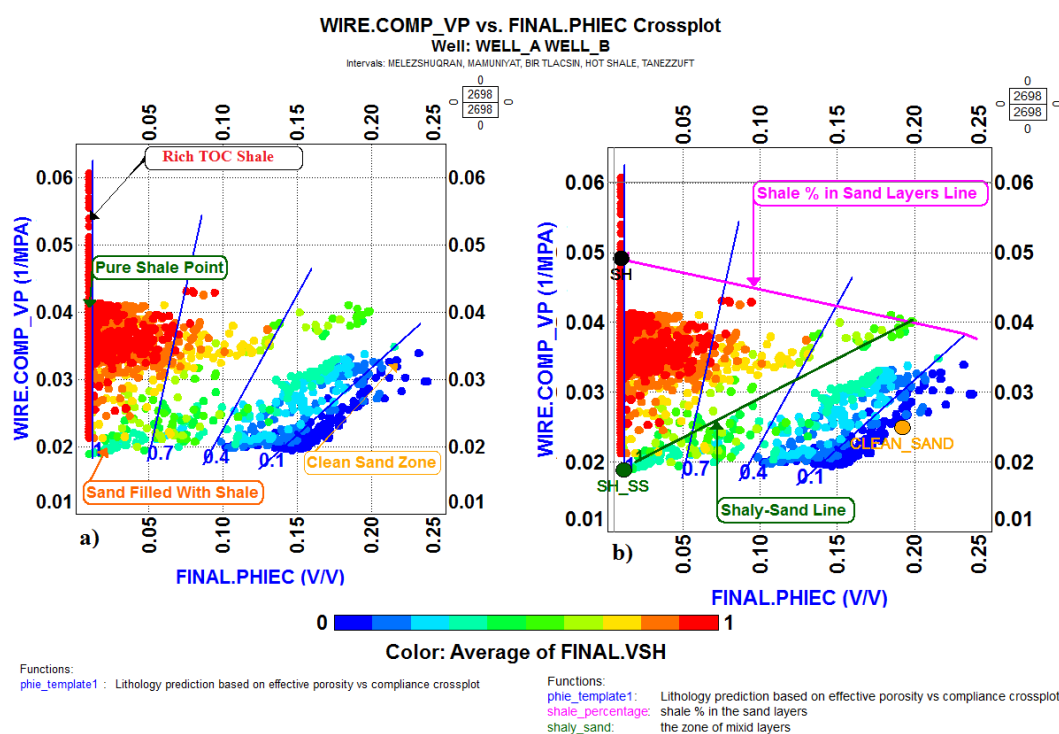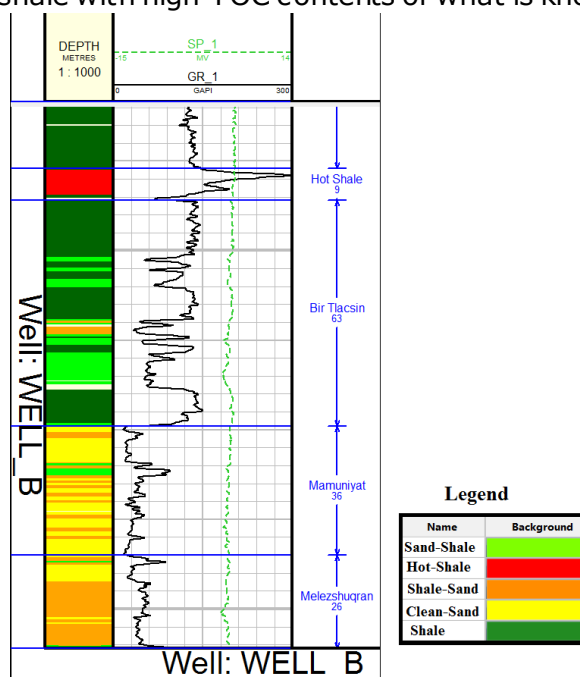

Fig. 8. A cross plot a) effective porosity versus compressional compliance log, b) is the same with a different template. The latter was used for lithology prediction illustrated in the lithology log. The figure represents the primary lithology end members and dispersed shale layers for different formation in the zone of interest of Well A and B

The cross-plot enhanced the ability to define the sandy-shale and shaly-sand layers range. Figure (8a) represents the trend of the main lithology end members drown by the annotated (0 to 1%) blue lines in which the compressional compliance increases in the areas with abundant shales and lower porosities (showed by v-sh colour coding red shale and blue sand). However, it slightly increases in the high porosity clean sandstone zones with shaly contents which can give an apparent difference between lower Ordovician formation "Melezshuqran"

and upper Ordovician Mamuniyat". Where they have similar porosities range (0.14 to 0.2 V/V), however the shale content of the former is higher, causing a rise of compressional compliance values (0.023-0.033 1/MPA) (Fig. 8a).

The cross-plot also led to the segregation of the three exist shales which is very hard to accomplish using traditional triple compo logging set. Since all the shale with high clay contents exhibits a very low porosity, the Vp-compliance log is used to differentiate between shale types. The first type is pure shale (Tanezzuft Fm) has a compressional compliance range of (0.028-0.033 1/MPA) that is decreasing with the increase of quartz contents and porosity. Then the shale with compressional compliance higher the 0.045 1/MPA is considered to be shale with high TOC contents or what is known in this area by "Hot shale" (Fig. 8).

Well: WELL_B

The last type is the controversial shale of the late Ordovician known as "Birtlacsin" which is often confused with lower Silurian Formation Tenezuft and the Upper Ordovician Mamuniyat reservoir. The formation (Birtlacsin) has a lower compliance than the fore-stated two types below 0.03 1/MPA which is due to the higher contents of the mixed layers than the pure shale in this formation (Fig. 8b). This observation outlined by the green shaly-sand line in figure (8b). The interpreted lithology log using the above cross-plot suggested a higher percentage of shaly-sand layers within the Upper Ordovician Mamuniyat reservoir overlain by sand-shale layers within the late Ordovician Birtlacsin formation (Fig. 9).

Fig. 9. Representing the prediction of different lithologies (Shale dark green, Sand yellow, sand-shale light green, shale-sand orange and hot-shale is red).using the cross plot of compressional compliance versus effective porosity

4.5. Compressional compliance versus velocity and Poisson's ratios cross-plots

The relationship between compressional compliance, poison's ratio and velocity ratio has been investigated in both wells. It was obtained by cross-plotting compressional compliance vs poison's ratio and colour-coded by the volume of shale (Fig. 10). The graph illustrated a consistent continuation of shale (red) and sand (blue) lithology end members, which bound the sand-shale layers (yellow to light green) and shale-sand lamination (light blue) (Fig. 10). The cross-plot was used to generate lithology log which has confirmed the result previously generated using compliance vs density but with a slight improvement in the layers number and type's distribution. The cross-plot of compliance versus Vp/Vs strongly supported the above lithology and contact separation obtained by poison's ratio (Fig. 11).

4.6. Facies prediction

The scheme for classifying the facies of Ordovician succession in this study is entirely based on the response of petrophysical and estimated elastic logs. The scheme classifies Ordovician deposits on the basis of shale percentages within sand layers and vice versa, organic matter contents and wireline log response. Five clusters have been recognized (Fig. 12), namely: (1) sandy-shale dominated layers (FA1), (2) TOC rich deposits (FA2), (3) shaly-sand dominated layers (FA3), (4) clean sand deposits (FA4), and (5) pure shale deposits (FA5). In Well A, only four petrophysical facies associations are present and (FA1) is missing, but in petro-elastic

facies the five clusters are present. While in Well B only three petrophysical facies are identified (FA2, FA4 and FA5), however, under the petro-elastic classification all the facies are present. In both wells, the petro-elastic facies shows a closer match to the litho-facies more than petrophysical facies (Fig. 12).
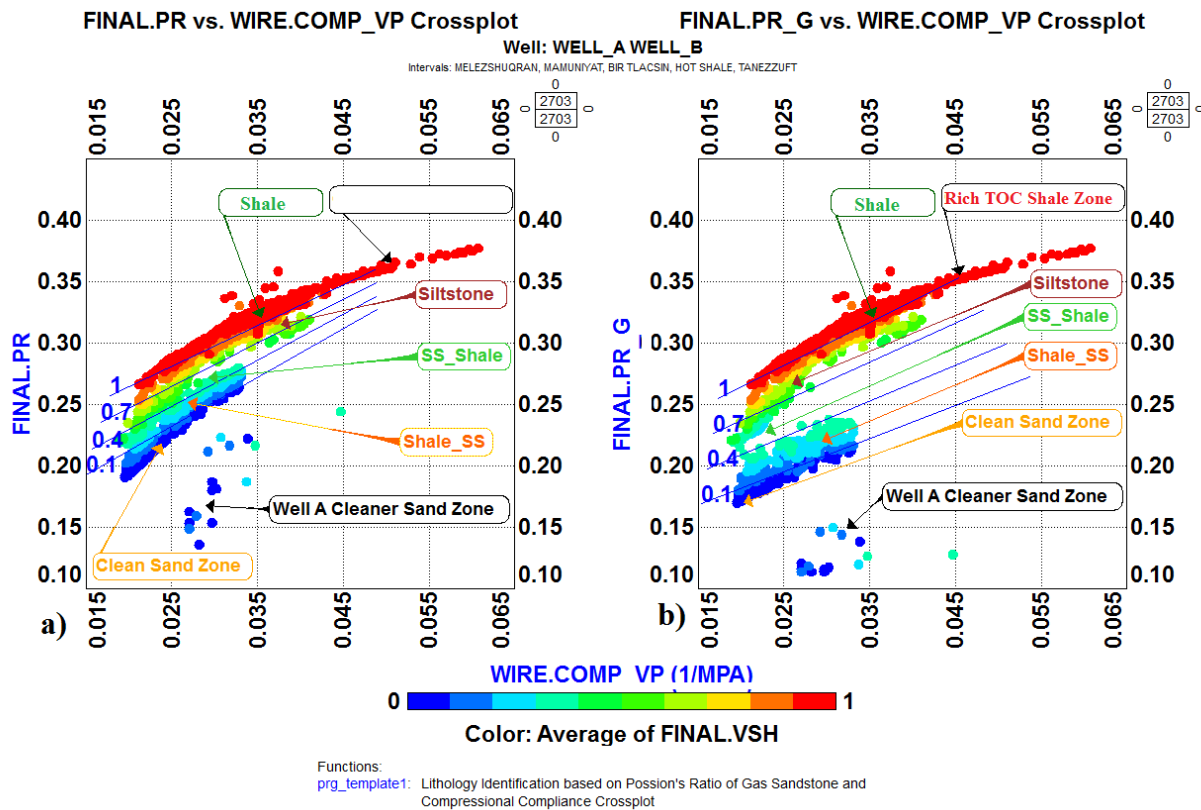

Fig. 10. A cross plot of compressional compliance versus Poisson's ratio (colour-coded by V-shale) showing the main lithology end members

5. Discussion

Precise delineation and understanding of lithology and facies are the primary keys to any successful exploration, appraisal and development operations. However, it still a fundamental obstacle for the subsurface operations [17]. Also, the profitability of any oil or gas field is reliant on the quality and correctness of lithology and associated facies prediction [18]. Before progressing with any elastic properties analysis, a robust estimation of shear wave velocity in all the wells is required. In this study, different methods (section 3.2.1) were tested and supervised neural network proved to be a powerful tool for shear wave estimation if suitable input logs were chosen (Fig. 3). Many input pairs were tested, and the set of gamma-ray, density, Vsh and total porosity logs was best predicted the shear wave with an almost overlay to the measured one in well A (Fig. 3). By investigating the different relation between estimated elastic and petrophysical properties and cross-plot them with each other, color-coded mainly by the volume of shale in the whole wells and zone of interest, it provides treasured information for facies and lithology, from which, also sandy-shale, shaly-sand and TOC content percentages are inferred. All the examined correlations allowed lithology primary end member separation. However, they lack a clear differentiation between the two kinds of thinly interbedded layers (shaly-sand and sandy-shale).

Well B exhibited more than ten thin layers ranging from (0.3-2 m) in thickness. Poison's ratio, velocity ratio and effective porosity cross-plots vs compressional compliance enhanced the allocation of the different lithological types within the zone of interest (Fig. 9, 10, and 11).

FINAL.VPVS_G vs. WIRE.COMP_VP Crossplot
Well: WELL_A WELL_B
Intervals: TANEZZUFT, HOT SHALE, BIR TLACSIN, MAMUNIYAT, MELEZSHUQRAN,
Filter:

FINAL.VPVS_G

WIRE.COMP_VP (1/MPA)

Color: Maximum of WIRE.LFP_VSH

Functions:
vpvps_compliance_lith: sandy_shale and shaly sand lithology sepration
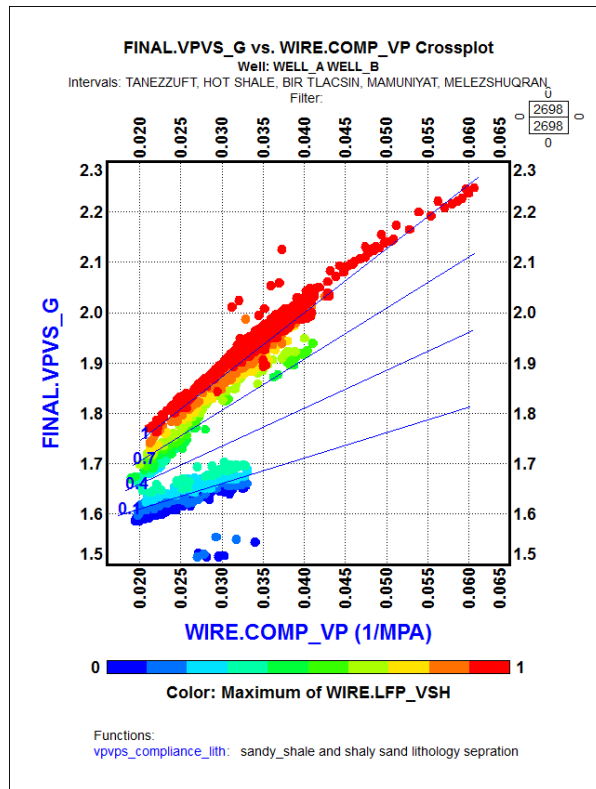
Fig. 11. A cross plot between A) compressional compliance versus VP/VS gas and B) compressional compliance versus VP/VS gas (colour-coded by V-shale) showing the main lithology end members

Shaly-sand fluid substitution for both wells manages to recognise some of the thin layers within shale and sand intervals. However, most of the layers identified within reservoir units have not been taking into account in the fluid substitution estimation. Therefore, erroneous results of fluid substitution application may occur. The "Mamuniyat" formation (main reservoir) with more clean sand content shows low compressional compliance, low-velocity ratio, and low Poisson's ratio. In contrary, the rich TOC shale (Hot shale) shows high compressional compliance, high-velocity ratio and high Poisson's ratio. While the debated sandstone, siltstones and silty shales of late Ordovician "Bir Tlacsin" formation has slightly higher compressional compliance, velocity ratio, and Poisson's ratio than the underlying Mamuniyat formation, which enables drawing a clear contact between two gradually graded formations in the areas with no abrupt changes (Fig. 9, 10, 11, and 12). The pure shale formation "Tanezzuft" has lower compressional compliance, velocity ratio, and Poisson's ratio than the rich TOC "Hot Shale" formation but higher values than the shale in the underlying Bir Tlacsin formation. This has enabled the separation of the three

shales (Hot sale, Tanezzuft shale and Bir Tlacsin shale) that often have a higher gamma-ray reading and appears very similar when only petrophysical properties are considered. The thinly interbedded sand and shale layers are bounded between two main identified end members (clean sand of Mamuniyat and pure shale of Tanezzuft formation) and if the percentage of shale increases in the sandy unit the above parameters will move towards the shale end member and vice versa.

According to Bhatt and Helle [3] the Application ANN in clastic rocks for facies prediction "reveals an average hit rate well above 90% in wells unknown to the network". in compression to the other methods the technique proved to be a reliable lithology and facies clustering method. Hence it was favoured in this study for petrophysical and petro-elastic facies prediction. Predicted petrophysical facies clusters in both wells failed to differentiate between the various type of shales as well as sandy-shale and shaly-sand layers (Fig. 12), where the facies association 2 (Hot shale) was considered to exist within the main reservoir unit, which is incorrect. This was due to the overlap between the petrophysical parameters of the clastic sediments and for minimizing its effect elastic properties are invoked in the analysis along with petrophysical properties. The facies is also significantly affected by the high gamma-ray reading in Well A, leading to misinterpretation and confusion of integrated sand-shale and shale layers. (FA3 and FA5).To overcome this issue, a combined petro-elastic facies cluster prediction using the earlier generated logs as input (Vp-compliance, Poisson's ratio, VPVS, PHIE and RHOB) is generated, the cluster accurately determines the Hot shale (FA2) and place it in the correct position within both wells (Fig. 12). Also, reliably delineated the interbedded sandy- shale and shaly-sand thin layers without using gamma-ray logs which have lowered the effect of petrophysical properties values interference for the lithological end members.

Finally, The unsupervised neural network predicted petro-elastic facies using logs (Poison's ratio, VpVs and effective porosity with compressional compliance) as an input showed a reasonable ability for detecting mixed shale sand layers than the only petrophysical logs (GR, NPHI, ROHB and PHI) clusters (Fig 12). Also illustrated a closer match to the litho-facies derived from mud logging.
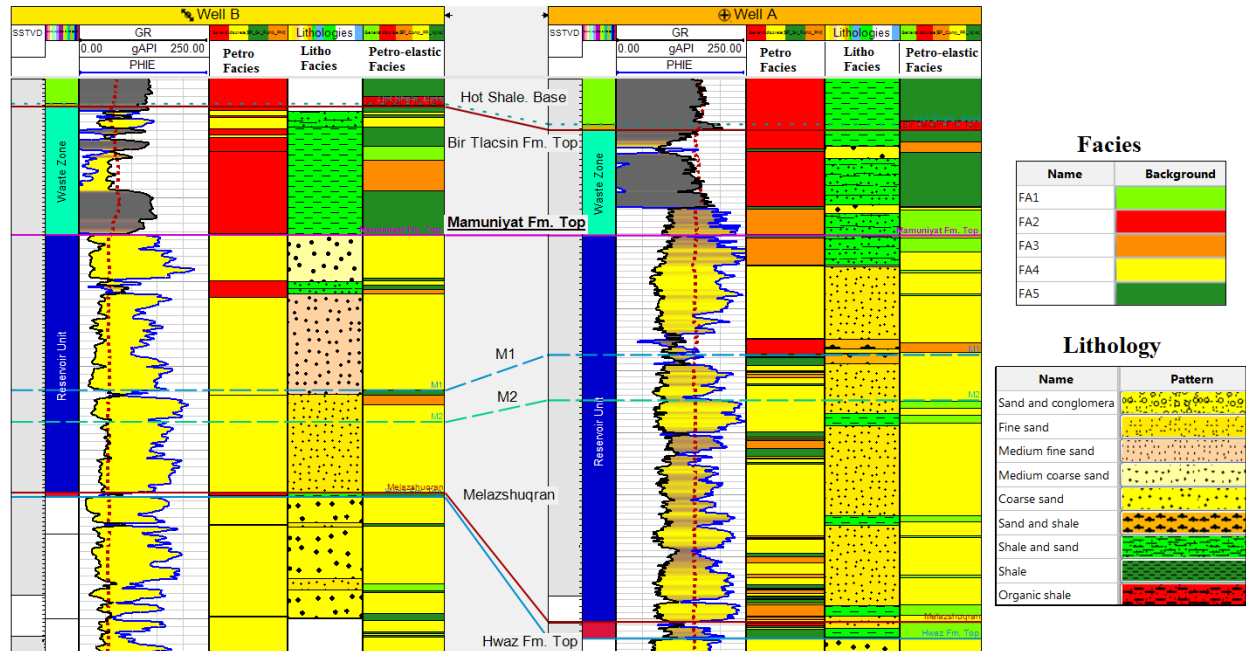

Fig. 12. Illustrate the predicted petrophysical and petro-elastic facies in comparison to the litho-facies for well A and well B

6. Conclusion

Even with the absence of high-resolution data such as image and core data, it is still possible to improve the determination of lithology and facies. In this study, a combination of petrophysical and elastic properties is correlated and used as an input for supervised and unsupervised neural network techniques in an attempt to improve the prediction of shear wave velocity, lithology and facies in the studied wells. The methods relied on a coupling of elastic and petrophysical properties to minimize the overlap of the petrophysical logs response to the clastic rocks. The supervised neural network analysis successfully improved the accuracy of VS estimation in Well B, where the measured one is absent. While the unsupervised neural network aided in the detection of different petrophysical facies clusters and significantly improved the delineation of the upper and lower boundaries of thinly interbedded sand and shale layers under the petro-elastic facies scheme. Application to an Ordovician succession of Murzuq basin revealed a precise five facies clusters. The outcome of this paper will help to improve sandy-shale fluid substitution, rock physics models reservoir model.

Acknowledgement

List of abbreviations

V_{sh}	Shale volume	C	Compressional compliance
GR_{log}	Gamma ray log reading	R_t	Deep resistivity
GR_{min}	Gamma ray sand reading	m	Cementation exponent
GR_{max}	Gamma ray shale reading	V_p	Compressional velocity
ϕ_N	Neutron Porosity from the logs	V_s	Shear velocity
ϕ_D	Density porosity	V_p/V_s	Velocity ratio
ρ_{ma}	Matrix density	K_{sat}	Bulk moduli of saturated rock
ρ_{log}	Bulk density from log	K_{dry}	Bulk moduli of the dry rock
ρ_{fl}	Fluid density	K_f	Bulk moduli of the fluid
ϕ_S	Sonic derived porosity	K_{ma}	Bulk moduli of the rock matrix
Δt_{ma}	Matrix transit time	S_w	Water saturation from logs
Δt_{log}	Sonic transit time from log	ρ_w	Density of formation water
Δt_{fl}	Fluid transit time	ρ_{hc}	Density of hydrocarbon
ϕ_{total}	Total Porosity	ρ_g	Density of formation gas
ϕ_{Seff}	Effective porosity	ρ_b	Bulk density
S_w	Water saturation	K_{hc}	Bulk moduli of hydrocarbon
n	Saturation exponent	μ_{sat}	Shear moduli of saturated rock
R_w	Brine resistivity	ρ_{sat}	Density of saturated rock
SD	Sand Stone	μ_{dry}	Shear moduli of dry roc
SH	Shale		

References

[1] Echikh K and Sola M. Geology and hydrocarbon occurrences in the Murzuq Basin, SW Libya. in Geological exploration in Murzuq Basin, ed: Elsevier, 2000, pp. 175-222.

[2] Abushalah Y and Serpa L. Using instantaneous frequency and colored inversion attributes to distinguish and determine the sandstones facies of the Late Ordovician Mamuniyat reservoir, R-field in Murzuq Basin, Libya. Interpretation, 2016; 4: T507-T519.

[3] Bhatt A and Helle HB. Determination of facies from well logs using modular neural networks. Petroleum Geoscience, 2002; 8: 217-228.

[4] Katahara K. Fluid substitution in laminated shaly sands. in SEG Technical Program Expanded Abstracts 2004, ed: Society of Exploration Geophysicists, 2004: 1718-1721.

[5] Dejtrakulwong P and Mavko G. Fluid substitution for laminated sand-shale sequences. in SEG Technical Program Expanded Abstracts 2011, ed: Society of Exploration Geophysicists, 2011, pp. 2183-2187.

[6] Aziz A. Stratigraphy and hydrocarbon potential of the Lower Palaeozoic succession of License NC-115, Murzuq Basin, SW Libya-Chapter 16. 2000.

[7] Davidson L, Beswetherick S, Craig J, Eales M, Fisher A, Himmali A. The structure, stratigraphy and petroleum geology of the Murzuq Basin, Southwest Libya-Chapter 14. 2009.

[8] Grothe B and Park TJ. Structure and function of the bat superior olivary complex. Microscopy Research and Technique, 2000; 51. 382-402.

[9] Najem A, El-Arnauti A, and Bosnina S. Delineation of Paleozoic Tecto-stratigraphic Complexities in the Northern Part of Murzuq Basin-Southwest Libya. in SPE North Africa Technical Conference and Exhibition, 2015.

[10] Le Heron D, Meinhold G, Elgadry M, Abutarruma Y, and Boote D. Early Palaeozoic evolution of Libya: perspectives from Jabal Eghei with implications for hydrocarbon exploration in Al Kufrah Basin. Basin Research, 2015; 27: 60-83.

[11] El-Ghali MAK. Depositional environments and sequence stratigraphy of paralic glacial, paraglacial and postglacial Upper Ordovician siliciclastic deposits in the Murzuq Basin, SW Libya. Sedimentary Geology, 2005; 177: 145-173.

[12] Shalbak FA. Palaeozoic petroleum systems of the Murzuq Basin, Libya. 2015.

[13] Asquith G. with CR Gibson. 1982, Basic Well Log Analysis for Geologist. AAPG Methods in Exploration Series, The American Assoc. of Petroleum Geologists, OK, 1986.

[14] Hill H, Klein G, Shirley O, Thomas E, and Waxman W. Bound Water In Shaly Sands-Its Relation To Q And Other Formation Properties. The log analyst, 1979; 20.

[15] Backus GE. Long-wave elastic anisotropy produced by horizontal layering. Journal of Geophysical Research, 1962; 67: 4427-4440.

[16]   Khalifa S, Laksana S, and Schöbel M. Rock Typing Approach for Reservoir Characterization of Ordovician Sandstones, Fields Case Study, Concessions NC115/NC186, Murzuq Basin, Libya. in North Africa Technical Conference and Exhibition, 2010.

[17]   Kupecz JA, Gluyas J, and Bloch S. Reservoir quality prediction in sandstones and carbonates: An overview. 1997.

[18]   Hami-Eddine K, Klein P, Richard L de Ribet, B, and Grout M. A new technique for lithology and fluid content prediction from prestack data: An application to a carbonate reservoir," Interpretation, 2015; 3: SC19-SC32.

To whom correspondence should be addressed: Dr. Abubaker Alansari, Department of Geosciences, University Technology PETRONAS, 32610, Perak, Malaysia